



Published in final edited form as:

Biochemistry. 2018 March 06; 57(9): 1517–1522. doi:10.1021/acs.biochem.7b01096.

Evidence of a General Acid/Base Catalysis Mechanism in the 8-17 DNAzyme

Marjorie Cepeda-Plaza¹, Claire E. McGhee², and Yi Lu^{2,*}

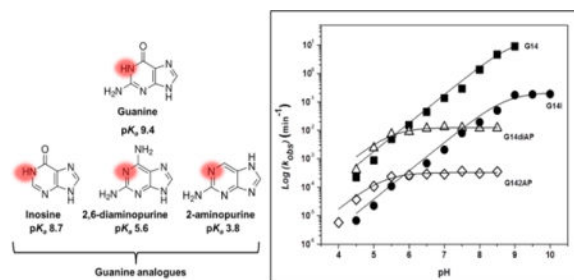
¹Department of Chemical Sciences, School of Exact Sciences, Universidad Andres Bello, República 275, Santiago, Chile

²Department of Chemistry, University of Illinois at Urbana-Champaign, 600 S. Mathews Ave., Urbana, Illinois 61801

Abstract

DNAzymes are catalytic DNA molecules which can perform a variety of reactions. Although advances have been made in obtaining DNAzymes via *in vitro* selection and many of them have been developed into sensors and imaging agents for metal ions, bacteria and other molecules, the structural features responsible for these enzymatic reactions are still not well understood. Previous studies of the 8-17 DNAzyme have suggested conserved guanines close to the phosphodiester transfer site may play a role in the catalytic reaction. To identify the specific guanine and functional group of the guanine responsible for the reaction, we herein report the effects of replacing G1.1 and G14 (G, $pK_{a,N1}$ 9.4) with analogs with a different pK_a at the N1 position, such as inosine (G14I, $pK_{a,N1}$ 8.7), 2,6-diaminopurine (G14diAP, N1 $pK_{a,N1}$ 5.6) and 2-aminopurine (G14AP, $pK_{a,N1}$ 3.8) on pH-dependent reaction rates. A comparison of the pH-dependence of the reaction rates of these DNAzymes demonstrated that G14 in the bulge loop, not G1.1 next to the cleavage site, is involved in proton transfer at the catalytic site. These results support general acid-base catalysis as a feasible strategy used in DNA catalysis, similar to RNA and protein enzymes.

TOC image



*Corresponding Author: Yi Lu, vi-lu@illinois.edu.

Notes

The authors declare no competing financial interests. Any additional relevant notes should be placed here.

INTRODUCTION

DNAzymes or deoxyribozymes are short single-stranded DNA molecules with catalytic properties.¹⁻⁷ Unlike naturally occurring ribozymes, DNAzymes have been obtained through *in vitro* selection, a combinatorial technique that obtains DNA molecules with preferred catalytic activity in the presence of a cofactor from a large library of sequences through iterative screening and amplification steps. Even though many DNAzymes have been obtained since their discovery in 1994,⁸ and some of them have been successfully developed into sensors and imaging agents for metal ions, bacteria and other targets,⁹⁻²⁵ the fundamental understanding of the structural features responsible for the catalytic activity and the reaction mechanisms of these DNAzymes has lagged behind.

Among DNAzymes, RNA-cleaving DNAzymes are the most studied group of this enzyme family.²⁶ These enzymes accelerate RNA cleavage by catalyzing an internal phosphodiester transfer reaction. The cleavage reaction is proposed to go through the internal nucleophilic attack of the phosphodiester bond by the 2'-oxygen on the ribose ring forming a pentacoordinated species, which evolves to form a 2',3'-cyclic phosphate and a 5'-hydroxyl terminal to the RNA fragment, similar to those of ribozymes.^{27, 28} The 8-17 DNAzyme is the most well-characterized member of the RNA-cleaving DNAzyme family. It has been obtained through multiple *in vitro* selection strategies carried out by different groups,²⁹⁻³² one variant of which is shown in Figure 1.³¹ This DNAzyme catalyzes a phosphodiester transfer reaction between a deoxyriboguanosine (G1.1) and a ribonucleotide adenosine (rA18, Figure 1A), on the substrate strand (red arrow, Figure 1).

To understand the reaction mechanism of this DNAzyme, various biochemical probing methods have been carried out.³²⁻⁴⁶ The 8-17 DNAzyme depends on divalent metal ions to perform catalysis. Even though the 8-17 DNAzyme was selected multiple times under different conditions and in the presence of different metal ions,²⁹⁻³² the highest activity observed is in the presence of Pb^{2+} , despite none of the *in vitro* selections being carried out in the presence of this metal ion. The activity rate of the 8-17 DNAzyme with respect to its divalent metal ion cofactor is in the order of $\text{Pb}^{2+} \gg \text{Zn}^{2+} \gg \text{Mn}^{2+} \approx \text{Co}^{2+} > \text{Ni}^{2+} > \text{Mg}^{2+} \approx \text{Ca}^{2+} > \text{Sr}^{2+} \approx \text{Ba}^{2+}$. Although the high specificity for Pb^{2+} has allowed for the development of highly selective sensors for this metal ion,⁹⁻¹² the functional and structural role of these metal cofactors in DNAzyme catalysis is not yet well understood, especially when compared with what is known about the interaction of metal ion with nucleic acids⁴⁷⁻⁵⁵ and ribozymes.⁵⁶⁻⁶⁴

The activity of the 8-17 DNAzyme is not only influenced by the identity of the divalent metal ion cofactor, but also by pH. Studies of the pH-profiles (rate constant vs pH) of the 8-17 DNAzyme in presence of Zn^{2+} ,³¹ Mg^{2+} ,³⁵ and Pb^{2+} ³⁶ have revealed a linear trend of $\log k_{obs}$ when the pH is increased, showing a slope close to 1.0, suggesting that a single proton transfer event is involved in the rate-limiting step of the reaction.³⁵ However, no studies have yet focused on evaluating proton transfer from specific functional groups at the catalytic core of the 8-17 DNAzyme.

Independent *in vitro* selections³² and mutational studies,^{34, 44} have allowed the identification of nucleotides essential for catalysis and conserved regions in the catalytic core of the 8-17 DNAzyme, including the G1.1•T2.1 wobble pair, located next to the cleavage site and the bulge loop, where C13 and G14 were identified as conserved nucleotides (Figure 1).³⁴ In addition, photo-cross-linking studies have revealed that G14 is in closest proximity to the cleavage site.⁴¹ These results have suggested that both G1.1 and G14 could participate in the catalytic mechanism employed by the 8-17 DNAzyme.

While the above studies have identified G1.1 and G14 as playing important roles in DNAzyme activity, the precise roles of the functional groups responsible for catalysis remain unknown. In contrast, numerous studies of ribozymes have elucidated the key roles several guanine residues play in general acid-base catalysis.^{64–77} For example, pH profile studies of the hairpin and hammerhead ribozyme have demonstrated that the N1 proton from guanine residues participate in general acid-base catalysis, even though its pK_a is far from the biological pH.^{67, 78, 79} Given the importance of the conserved G1.1 and G14 in catalysis, we herein use a method previously employed in the study of ribozymes by replacing G1.1 and G14 (G, $pK_{a,N1} = 9.4$) with its analogs with different pK_a values at the N1 position, i.e., inosine (G14I, $pK_{a,N1} = 8.7$), 2,6-diaminopurine (G14diAP, $pK_{a,N1} = 5.6$) and 2-aminopurine (G14AP, $pK_{a,N1} = 3.8$), in the interest of covering a wide pK_a range of the N1 imino proton.^{78, 79} It has been shown that the 8-17 DNAzyme is active in the presence of Mg^{2+} , Ca^{2+} , Zn^{2+} and Pb^{2+} .^{6, 9, 31, 35} We choose Mg^{2+} for this study, because it is the most soluble 8-17 DNAzyme metal ion cofactor over the widest range of pH conditions, which gives the opportunity to obtain the most complete pH profile and thus pK_a . A comparison of the pH-rate profiles found for the wild type DNAzyme and its variants has led us to suggest that G14, not G1.1, is involved in a general acid-base catalytic strategy in the mechanism of the 8-17 DNAzyme.

MATERIALS AND EXPERIMENTAL DETAILS

All oligonucleotides were obtained from Integrated DNA Technologies, Inc. (Coralville, IA). The wild type sequences were purified by polyacrylamide gel electrophoresis (PAGE) for kinetic assays and uranyl photocleavage, meanwhile the modified sequences were purchased in HPLC purified form. [γ -³²P]-adenosine 5'-triphosphate (ATP) was purchased from Perkin Elmer (Waltham, MA) and T4 kinase was purchased from New England Biolabs, Inc., (Ipswich, MA). All other chemicals were of at least ACS reagent grade and were purchased from either Sigma-Aldrich (St. Louis, MO), Thermo Fisher Scientific, Inc. (Waltham, MA) or Alfa-Aesar (Ward Hill, MA). Uranyl Nitrate hexahydrate was purchased from Fischer Scientific. All other metal salts used were obtained from Alfa-Aesar and were of Puratronic[®] grade (99.999% pure).

Kinetic assays

The substrate oligonucleotide (17S) was labeled at the 5'-end with [γ -³²P]-ATP using T4 kinase, purified on a C18 Sep-Pak[®] cartridge (Waters Corporation, Milford, MA), and stored at $-20^{\circ}C$. All kinetic assays were carried out at room temperature under single-turnover conditions with 4 μM enzyme and 2 nM substrate, in a buffer containing 50 mM acetate (pH

4.0 to 5.0), 50 mM MES (pH 5.5 to 6.5), 50 mM MOPS (pH 6.75 to 7.0), 50 mM HEPES (pH 7.25 to 8.0), and 50 mM Tris (pH 8.5 and 9.0) and 100 mM NaNO₃. Each buffer was incubated with Chelex 100 resin to remove trace metal ion impurities. The sample solution containing the enzyme and substrate in buffer was denatured at 95°C in a water bath for 3 minutes and then annealed by gradually cooling the container to room temperature over ~ 30 minutes. After annealing the solution, a 2 µL aliquot was added to 10 µL of stop solution containing 8 M urea, 50mM EDTA, 1 × TBE, and 0.05 % w/v each of bromophenol blue and xylene cyanol in a 96-well plate. This was the ‘zero-point’ control before the initiation of the reaction. Thereafter, appropriate volumes of MgCl₂ solutions were added to the sample to initiate the reaction and 2 µL aliquots were taken at suitable time intervals and added to the stop solution to end the reaction on the same 96-well plate. A final Mg²⁺ concentration of 20 mM was used for all activity assays. A denaturing 20% polyacrylamide gel was used to separate the uncleaved substrate and the cleaved product. Gel imaging was performed on a Molecular Dynamics Storm 430 phosphorimager, and quantified using Image-Quant software (GE Healthcare, UK). The percent of cleavage product at time ‘t’ was calculated by taking the ratio of the 5’-cleaved product to the total of the cleaved product and the uncleaved substrate, after subtraction of the background radioactivity on the gel. Kinetic plots were created using Origin 8.5 software (OriginEab Corporation, North-ampton, MA) and fit to the equation

$$P_t = \%P_0 + \%P_\infty(1 - e^{-kt}) \quad (1)$$

where % P₀ is the initial amount of product (at time, $t = 0$), % P_∞ is the amount of product formed at the endpoint plus the initial amount of product of the reaction (at $t = \infty$), % P_t is the amount of product at time t, and $k = k_{obs}$, the observed rate constant under single turnover conditions. All reported values are the average of at least two trials.

RESULTS AND DISCUSSION

The RNA-cleavage reaction rates, catalyzed by the 8-17 DNAzyme and its variants containing G14 analogs, were measured under single-turnover conditions in presence of 20 mM MgCl₂ in 50 mM buffer, 100 mM NaNO₃ between pH 4-10. Figure 2 shows log k_{obs} of the 8-17 DNAzyme at different pH conditions. This pH-rate profile reveals a linear trend with a slope of 1.02 and an incipient plateau at a pH close to 9, consistent with previously reported results.^{31, 35, 36} Having reproduced the pH profile of the wild type 8-17 DNAzyme, we measured the dependence of k_{obs} on the pH after substituting G14 with its analogs with lower pK_a values at the N1 imino proton to find out if the N1 proton of this G14 is involved in general acid-base catalysis. As shown in Figure 2, the 17E-G14I mutant shows a decreased cleavage rate and the linear dependency on the pH remains until a pH around 8.5, displaying a slope of 0.99. Above pH 8.5, the rate of cleavage is almost constant. Interestingly, below pH 5.5, replacing wild type G14 with the 2,6-diaminopurine analog (17E-G14diAP) did not have a significant impact on the 8-17 DNAzyme activity. Above pH 5.5, however, this mutation lowered the activity dramatically by one to three orders of magnitudes, reaching a plateau at conditions over a pH of 6. Finally, the 17E-G14AP mutant

displayed a pH-rate profile almost parallel to the one found for the 17E-G14diAP construct, except for the fact that the overall activity was decreased by two orders of magnitudes.

The changes observed in the pH-rate profiles of the 8-17 DNAzyme, caused by the introduction of the guanine analogs, reveal the influence of the N1 imino proton on the catalytic activity of the enzyme. When the pK_a of the N1 is considerably decreased, such as in the case of G14diAP and G14AP, the mutation leads to a plateau in the catalytic profile of the enzyme at pH conditions higher than its pK_a . Interestingly, the calculated pK_a of the 8-17 DNAzyme and the G14 variants are in good agreement with the pK_a values of the free bases. Figure 3 shows the correlation between the calculated pK_a of the 17E-G14 mutant and the pK_a of the free base. These results suggest the participation of the G14 N1 in proton transfer.^{56, 67}

Two possible scenarios could account for the observed catalytic behavior. The first is that G14 is acting as a general acid. In this situation, when N1 is deprotonated over its pK_a , this functional group is no longer available to perform proton transfer. If G14 is acting as a general acid, it would imply the existence of a general base with a pK_a over 10. The second possibility is that G14 operates as a general base. In this case, over the pK_a of the N1, the base would be completely deprotonated and therefore fully capable of executing proton transfer. Consequently, G14 would no longer contribute to the acceleration of the cleavage reaction.^{56, 67} This model would be consistent with the catalytic strategy used by different ribozymes such as the hairpin and the hammerhead⁷⁹ ribozymes or the recently discovered twister^{73, 77} and Varkud satellite⁷⁵ ribozymes, in which a conserved guanine residue plays a direct role in proton transfer as a general base.

The results reported here for the 8-17 DNAzyme are similar to those previously reported for the hairpin and the hammerhead ribozymes. Pinard *et al.* evaluated the role of the conserved guanine residue located at position 8 in acid-base catalysis for the hairpin ribozyme. By constructing the pH-rate profiles of G8 mutants using analogs inosine, 2,6-diaminopurine and 2-aminopurine, they found that activity was influenced by the pH in some variants.⁷⁸ In another study, Han *et al.* mutated conserved G5, G8 and G12 at the catalytic core of hammerhead ribozyme using the same guanine analogs, and showed that, while the individual substitution of bases G5, G8, or G12 produced some level of inhibition, G5 variants were inhibited independent of pH, while G8 and G12 mutations showed pH-dependent inhibition. The most dramatic effect was observed when G8 and G12 were simultaneously mutated, showing a markedly different pH-dependence.⁷⁹ In both studies, when the corresponding guanine residue was replaced with inosine, a pH-rate profile similar to the wild type ribozyme was observed, except the overall k_{obs} values were much lower than those of wild type ribozymes. In contrast, they found that the introduction of 2,6-diaminopurine and 2-aminopurine displayed a pH-dependent activity, different from the profile of wild type ribozymes.^{78, 79} These results revealed the direct role of guanine residues in acid-base catalysis in the hairpin ribozyme and the hammerhead ribozyme, respectively. The similarities between our results and those reported for these ribozymes support the direct role of the guanine residue G14 in general acid-base catalysis in the 8-17 DNAzyme.

While this work was under review, Liu *et al.* reported the first crystal structure of the 8-17 DNAzyme. While the sequence and conditions in which the crystal was obtained are not identical to ours, structural information revealed from the crystal structural study also suggests that G14 operates as a general base. Liu *et al.* obtained the 8-17 DNAzyme crystal structure with the ribonucleotide active site replaced by a deoxyribonucleotide in one construct and protected with a 2'-OMe-G modification to improve the DNAzyme stability during data collection in a second construct.⁸⁰ The crystal structure confirms a variety of biochemical assays that previously revealed the close proximity of certain conserved residues to the cleavage site.^{34, 41} In the pre-catalytic structure of the 2'-OMe-G modified construct, an alignment between the nucleophilic 2'-O and the electrophilic P of the phosphate of the 2'-OMe-G modified ribonucleotide is observed. This structure suggests that phosphodiester transesterification occurs through an in-line attack by the 2'-O of the phosphate located at the cleavage site. Furthermore, G14 (named G13 in the crystal structural study) appears to form a non-canonical base pairing with A6 (named A5 in the crystal structural study). This unusual interaction induces a conformation that enables the N1 of G14 to be located close to the 2'-O, possibly activating the nucleophilic 2'-O by acting as a general base.

Encouraged by the results of probing G14 at the catalytic core of the 8-17 DNAzyme-substrate complex, in addition to previous evidence that has shown the relevance of G1.1 located at the cleavage site, we replaced wild type G1.1 with its analog 2,6-diaminopurine (G1.1diAP). We found that, although the pH profile of this construct was strongly shifted down (Figure 4), the activity profile did not reveal any disruption from linearity over the range of pH conditions studied, in contrast to what was observed when the same analog was introduced at G14 in the enzyme strand. The lack of influence by pH over the activity of this construct does not support the participation of the N1 from G1.1 in protonation events in the reaction of the 8-17 DNAzyme. Recently reported structural data also confirms that G1.1 and T2.1 (named G+1 and T1, respectively in the crystal structural study) form a wobble base-pairing. According to Liu *et al.* this pairing, in conjunction with a noncanonical pairing between the ribonucleotide and A15 (referred to as A14 in the crystal structural study), forms a kink between G1.1 and the ribonucleotide exposing the 2'-O of the 2'-OMe-G modified construct and favoring the formation of the DNAzymes catalytic conformation.⁸⁰ Furthermore, the crystal structure reveals that the N1 of G1.1 interacts with the O2 of T2.1, and therefore would not be available to participate in proton transfer as shown in our results. Consequently, the severe drop in the activity of 17E/S-G1.1diAP compared to the wild type can be explained by the disruption of the G•T wobble pair since the carbonyl group on guanosine responsible for interacting with the N3 of T2.1 is replaced with an amine group.

CONCLUSION

While a large body of work has been focused on *in vitro* selection and the application of DNAzymes as sensors and imaging agents, the structural features and reaction mechanisms employed by these DNAzymes to accelerate reactions, such as phosphodiester bond cleavage, remain poorly understood. In this study, we have found that the N1 imino proton of the guanine residue located at position 14, plays a direct role in the catalytic activity of the 8-17 DNAzyme, probably by being involved in a proton transfer event. These results are

in good agreement with the recently reported crystal structure of this enzyme and allow for deeper insight into the structural features and the mechanism for this class of DNAzymes.

Acknowledgments

This material is based upon work supported by the National Institutes of Health (GM124316), CONICYT Chile (79130030) and FONDECYT Chile (11140401).

Funding Sources

This material is based upon work supported by the National Institutes of Health (GM124316 and MH110975), CONICYT Chile (79130030) and FONDECYT Chile (11140401)

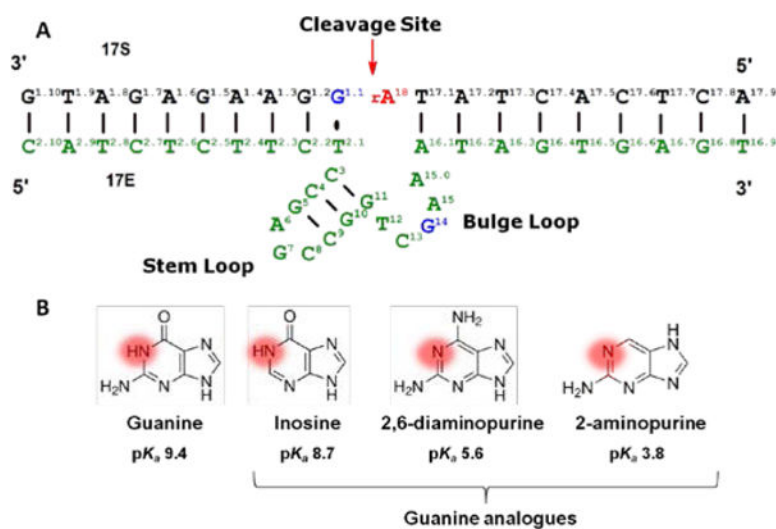
References

1. Peracchi A. DNA Catalysis: Potential, Limitations, Open Questions. *ChemBioChem*. 2005; 6:1316–1322. [PubMed: 16003806]
2. Silverman SK. Deoxyribozymes: selection design and serendipity in the development of DNA catalysts. *Acc Chem Res*. 2009; 42:1521–1531. [PubMed: 19572701]
3. Schlosser K, Li Y. Biologically Inspired Synthetic Enzymes Made from DNA. *Chem Biol*. 2009; 16:311–322. [PubMed: 19318212]
4. Hollenstein M. DNA Catalysis: The Chemical Repertoire of DNAzymes. *Molecules*. 2015; 20:20777–20804. [PubMed: 26610449]
5. Silverman SK. Catalytic DNA: Scope, Applications, and Biochemistry of Deoxyribozymes. *Trends Biochem Sci*. 2016; 41:595–609.
6. Lu Y. New Transition-Metal-Dependent DNAzymes as Efficient Endonucleases and as Selective Metal Biosensors. *Chem - Em- J*. 2002; 8:4588–4596.
7. Linns HE, Lu Y. In Vitro Selection of Metal-Ion-Selective DNAzymes. *Methods Mol Biol*. 2012; 848:297–316. [PubMed: 22315076]
8. Breaker RR, Joyce GF. A DNA enzyme that cleaves RNA. *Chem Biol*. 1994; 1:223–229. [PubMed: 9383394]
9. Li J, Lu Y. A highly sensitive and selective catalytic DNA biosensor for lead ions. *J Am Chem Soc*. 2000; 122:10466–10467.
10. Liu J, Lu Y. A colorimetric lead biosensor using DNAzyme-directed assembly of gold nanoparticles. *J Am Chem Soc*. 2003; 125:6642–6643. [PubMed: 12769568]
11. Lan T, Furuya K, Lu Y. A highly selective lead sensor based on a classic lead DNAzyme. *Chem Commun*. 2010; 46:3896–3898.
12. McGhee CE, Loh KY, Lu Y. DNAzyme sensors for detection of metal ions in the environment and imaging them in living cells. *Curr Opin Biotechnol*. 2017; 45:191–201. [PubMed: 28458112]
13. Liu J, Brown AK, Meng X, Cropek DM, Istok JD, Watson DB, Lu Y. A catalytic beacon sensor for uranium with parts-per-trillion sensitivity and millionfold selectivity. *Proc Natl Acad Sci U S A*. 2007; 104:2056–2061. [PubMed: 17284609]
14. Hollenstein M, Hipolito C, Lam C, Dietrich D, Perrin DM. A Highly Selective DNAzyme Sensor for Mercuric Ions. *Angew Chem, Int Ed*. 2008; 47:4346–4350.
15. Ali MM, Aguirre SD, Lazim H, Li Y. Fluorogenic DNAzyme Probes as Bacterial Indicators. *Angew Chem, Int Ed*. 2011; 50:3751–3754.
16. Xiang Y, Lu Y. DNA as Sensors and Imaging Agents for Metal Ions. *Inorg Chem*. 2014; 53:1925–1942. [PubMed: 24359450]
17. Hwang K, Wu P, Kim T, Lei L, Tian S, Wang Y, Lu Y. Photocaged DNAzymes as a General Method for Sensing Metal Ions in Living Cells. *Angew Chem, Int Ed*. 2014; 53:13798–13802.
18. Torabi SF, Wu P, McGhee CE, Chen L, Hwang K, Zheng N, Cheng J, Lu Y. In vitro selection of a sodium-specific DNAzyme and its application in intracellular sensing. *Proc Natl Acad Sci U S A*. 2015; 112:5903–5908. [PubMed: 25918425]

19. Gong L, Zhao Z, Lv YF, Huan SY, Fu T, Zhang XB, Shen GL, Yu RQ. DNAzyme-based biosensors and nanodevices. *Chem Commun.* 2015; 51:979–995.
20. Zhang J, Cheng F, Li J, Zhu JJ, Lu Y. Fluorescent nanoprobe for sensing and imaging of metal ions: Recent advances and future perspectives. *Nano Today.* 2016; 11:309–329. [PubMed: 27818705]
21. Zhang W, Feng Q, Chang D, Tram K, Li Y. In vitro selection of RNA-cleaving DNAzymes for bacterial detection. *Methods.* 2016; 106:66–75. [PubMed: 27017912]
22. Wang W, Satyavolu NSR, Wu Z, Zhang JR, Zhu JJ, Lu Y. Near-Infrared Photothermally Activated DNAzyme–Gold Nanoshells for Imaging Metal Ions in Living Cells. *Angew Chem, Int Ed.* 2017; 56:6798–6802.
23. Wu Z, Fan H, Satyavolu NSR, Wang W, Lake R, Jiang JH, Lu Y. Imaging Endogenous Metal Ions in Living Cells Using a DNAzyme–Catalytic Hairpin Assembly Probe. *Angew Chem, Int Ed.* 2017; 56:8721–8725.
24. Liu M, Chang D, Li Y. Discovery and Biosensing Applications of Diverse RNA-Cleaving DNAzymes. *Acc Chem Res.* 2017; 50:2273–2283. [PubMed: 28805376]
25. Zhou W, Saran R, Liu J. Metal Sensing by DNA. *Chem Rev.* 2017; 117:8272–8325. [PubMed: 28598605]
26. Silverman SK. In vitro selection, characterization, and application of deoxyribozymes that cleave RNA. *Nucleic Acids Res.* 2005; 33:6151–6163. [PubMed: 16286368]
27. Breaker RR, Emilsson GM, Lazarev D, Nakamura S, Puskarz IJ, Roth A, Sudarsan N. A common speed limit for RNA-cleaving ribozymes and deoxyribozymes. *RNA.* 2003; 9:949–957. [PubMed: 12869706]
28. Emilsson GM, Nakamura S, Roth A, Breaker RR. Ribozyme speed limits. *RNA.* 2003; 9:907–918. [PubMed: 12869701]
29. Santoro SW, Joyce GF. A general purpose RNA-cleaving DNA enzyme. *Proc Natl Acad Sci U S A.* 1997; 94:4262–4266. [PubMed: 9113977]
30. Faulhammer D, Famulok M. Characterization and divalent metal-ion dependence of in vitro selected deoxyribozymes which cleave DNA/RNA chimeric oligonucleotides. *J Mol Biol.* 1997; 269:188–202. [PubMed: 9191064]
31. Li J, Zheng W, Kwon AH, Lu Y. In vitro Selection and Characterization of a Highly Efficient Zn(II)-dependent RNA-cleaving Deoxyribozyme. *Nucleic Acids Res.* 2000; 28:481–488. [PubMed: 10606646]
32. Cruz RPG, Withers JB, Li Y. Dinucleotide junction cleavage versatility of 8-17 deoxyribozyme. *Chem Biol.* 2004; 11:57–67. [PubMed: 15112995]
33. Leung EKY, Sen D. Electron Hole Flow Patterns through the RNA-Cleaving 8-17 Deoxyribozyme Yield Unusual Information about Its Structure and Folding. *Chem Biol.* 2007; 14:41–51. [PubMed: 17254951]
34. Peracchi A, Bonaccio M, Clerici M. A Mutational Analysis of the 8-17 Deoxyribozyme Core. *J Mol Biol.* 2005; 352:783–794. [PubMed: 16125199]
35. Bonaccio M, Credali A, Peracchi A. Kinetic and thermodynamic characterization of the RNA-cleaving 8–17 deoxyribozyme. *Nucleic Acids Res.* 2004; 32:916–925. [PubMed: 14963261]
36. Brown AK, Li J, Pavot CMB, Lu Y. A Lead-Dependent DNAzyme with a Two-Step Mechanism. *Biochem.* 2003; 42:7152–7161. [PubMed: 12795611]
37. Kim HK, Rasnik I, Liu J, Ha T, Lu Y. Dissecting metal ion-dependent folding and catalysis of a single DNAzyme. *Nat Chem Biol.* 2007; 3:763–768. [PubMed: 17965708]
38. Lee NK, Koh HR, Han KY, Kim SK. Folding of 8-17 deoxyribozyme studied by three-color alternating-laser excitation of single molecules. *J Am Chem Soc.* 2007; 129:15526–15534. [PubMed: 18027936]
39. Kim HK, Li J, Nagraj N, Lu Y. Probing Metal Binding in the 8-17 DNAzyme by Tb(III) Luminescence Spectroscopy. *Chem - Eur J.* 2008; 232:8696–8703.
40. Schlosser K, Gu J, Sule L, Li Y. Sequence-function relationships provide new insight into the cleavage site selectivity of the 8–17 RNA-cleaving deoxyribozyme. *Nucleic Acids Res.* 2008; 36:1472–1481. [PubMed: 18203744]

41. Liu Y, Sen D. A contact photo-cross-linking investigation of the active site of the 8-17 deoxyribozyme. *J Mol Biol.* 2008; 381:845–859. [PubMed: 18586041]
42. Mazumdar D, Nagraj N, Kim HK, Meng X, Brown AK, Sun Q, Li W, Lu Y. Activity, Folding and Z-DNA Formation of the 8-17 DNAzyme in the Presence of Monovalent Ions. *J Am Chem Soc.* 2009; 131:5506–5515. [PubMed: 19326878]
43. Liu Y, Sen D. Local rather than global folding enables the lead-dependent activity of the 8-17 deoxyribozyme: evidence from contact photocrosslinking. *J Mol Biol.* 2010; 395:234–241. [PubMed: 19917290]
44. Wang B, Cao L, Chiuman W, Li Y, Xi Z. Probing the Function of Nucleotides in the Catalytic Cores of the 8–17 and 10–23 DNAzymes by Abasic Nucleotide and C3 Spacer Substitutions. *Biochem.* 2010; 49:7553–7562. [PubMed: 20698496]
45. Lam JC, Li Y. Influence of cleavage site on global folding of an RNA-cleaving DNAzyme. *ChemBioChem.* 2010; 11:1710–1719. [PubMed: 20665772]
46. Nakano SI, Watabe T, Sugimoto N. Modulation of Ribozyme and Deoxyribozyme Activities Using Tetraalkylammonium Ions. *ChemPhysChem.* 2017; 18:3614–3619. [PubMed: 28940937]
47. Barton J, Lippard S. Heavy metal interactions with nucleic acids. *Metal Ions in Biol.* 1980; 1:31–113.
48. Feig, AL., Uhlenbeck, OC. The role of metal ions in RNA biochemistry. In: Gesteland, RF, Cech, TR., Atkins, JF., editors. *The RNA World.* Cold Spring Harbor Laboratory Press; New York: 1999. p. 287
49. Guo Z, Sadler PJ. Metals in medicine. *Angew Chem, Int Ed.* 1999; 38:1512–1531.
50. Boerner LJK, Zaleski JM. Metal complex–DNA interactions: from transcription inhibition to photoactivated cleavage. *Curr Opin Chem Biol.* 2005; 9:135–144. [PubMed: 15811797]
51. Lippert, B. Coordinative Bond Formation Between Metal Ions and Nucleic Acid Bases. In: Hud, NV., editor. *RSC Biomolecular Sciences.* Royal Soc Chemistry; Cambridge: 2009. p. 39-74.
52. Sigel RK, Sigel H. A stability concept for metal ion coordination to single-stranded nucleic acids and affinities of individual sites. *Acc Chem Res.* 2010; 43:974–984. [PubMed: 20235593]
53. Pechlaner, M., Sigel, RKO. Characterization of Metal Ion-Nucleic Acid Interactions in Solution. In: Sigel, A., Sigel, H., Sigel, RK., editors. *Interplay between Metal Ions and Nucleic Acids.* Springer; Netherlands, Dordrecht: 2012. p. 1-42.
54. Muhammad N, Guo Z. Metal-based anticancer chemotherapeutic agents. *Curr Opin Chem Biol.* 2014; 19:144–153. [PubMed: 24608084]
55. Ward WL, Plakos K, DeRose VJ. Nucleic Acid Catalysis: Metals, Nucleobases, and Other Cofactors. *Chem Rev.* 2014; 114:4318–4342. [PubMed: 24730975]
56. Nakano S-I, Chadalavada DM, Bevilacqua PC. General Acid-Base Catalysis in the Mechanism of a Hepatitis Delta Virus Ribozyme. *Science.* 2000; 287:1493–1497. [PubMed: 10688799]
57. DeRose VJ. Metal Ion binding to catalytic RNA molecules. *Curr Opin Struct Biol.* 2003; 13:317–324. [PubMed: 12831882]
58. Sigel RKO, Pyle AM. Alternative Roles for Metal Ions in Enzyme Catalysis and the Implications for Ribozyme Chemistry. *Chem Rev.* 2007; 107:97–113. [PubMed: 17212472]
59. Nakano, S., Kitagawa, Y., Karimata, HT., Sugimoto, N. *Nucleic Acids Symposium Series.* Oxford Univ Press; Oxford: 2008. Molecular crowding effect on metal ion binding properties of the hammerhead ribozyme; p. 519-520.
60. Frederiksen JK, Piccirilli JA. Identification of catalytic metal ion ligands in ribozymes. *Methods.* 2009; 49:148–166. [PubMed: 19651216]
61. Sigel, A., Sigel, H., Sigel, RKO. *Structural and Catalytic Roles of Metal Ions in RNA.* Vol. 9. Royal Soc Chemistry; Cambridge: 2011.
62. Chen J, Ganguly A, Miswan Z, Hammes-Schiffer S, Bevilacqua PC, Golden BL. Identification of the Catalytic Mg²⁺ Ion in the Hepatitis Delta Virus Ribozyme. *Biochem.* 2013; 52:557–567. [PubMed: 23311293]
63. Denesyuk NA, Thirumalai D. How do metal ions direct ribozyme folding? *Nat Chem.* 2015; 7:793–801. [PubMed: 26391078]

64. Chen H, Giese TJ, Golden BL, York DM. Divalent Metal Ion Activation of a Guanine General Base in the Hammerhead Ribozyme: Insights from Molecular Simulations. *Biochem*. 2017; 56:2985–2994. [PubMed: 28530384]
65. Chowrira BM, Berzal-Herranz A, Burke JM. Novel guanosine requirement for catalysis by the hairpin ribozyme. *Nature*. 1991; 354:320–322. [PubMed: 1956383]
66. Rupert PB, Ferre-D'Amare AR. Crystal structure of a hairpin ribozyme-inhibitor complex with implications for catalysis. *Nature*. 2001; 410:780–786. [PubMed: 11298439]
67. Bevilacqua PC. Mechanistic Considerations for General Acid–Base Catalysis by RNA: Revisiting the Mechanism of the Hairpin Ribozyme†. *Biochem*. 2003; 42:2259–2265. [PubMed: 12600192]
68. Heldenbrand H, Janowski PA, Giamba u G, Giese TJ, Wedekind JE, York DM. Evidence for the Role of Active Site Residues in the Hairpin Ribozyme from Molecular Simulations along the Reaction Path. *J Am Chem Soc*. 2014; 136:7789–7792. [PubMed: 24842535]
69. Klein DJ, Been MD, Ferré-D'Amare AR. Essential Role of an Active-Site Guanine in glmS Ribozyme Catalysis. *J Am Chem Soc*. 2007; 129:14858–14859. [PubMed: 17990888]
70. Zhang S, Ganguly A, Goyal P, Bingaman JL, Bevilacqua PC, Hammes-Schiffer S. Role of the Active Site Guanine in the glmS Ribozyme Self-Cleavage Mechanism: Quantum Mechanical/Molecular Mechanical Free Energy Simulations. *J Am Chem Soc*. 2015; 137:784–798. [PubMed: 25526516]
71. Scott, WG., Horan, LH., Martick, M. Chapter One - The Hammerhead Ribozyme: Structure, Catalysis, and Gene Regulation. In: Soukup, GA., editor. *Progress in Molecular Biology and Translational Science*. Academic Press; 2013. p. 1-23.
72. Schultz EP, Vasquez EE, Scott WG. Structural and catalytic effects of an invariant purine substitution in the hammerhead ribozyme: implications for the mechanism of acid-base catalysis. *Acta Crystallogr D Biol Crystallogr*. 2014; 70:2256–2263. [PubMed: 25195740]
73. Liu Y, Wilson TJ, McPhee SA, Lilley DMJ. Crystal structure and mechanistic investigation of the twister ribozyme. *Nat Chem Biol*. 2014; 10:739–744. [PubMed: 25038788]
74. Gaines CS, York DM. Ribozyme Catalysis with a Twist: Active State of the Twister Ribozyme in Solution Predicted from Molecular Simulation. *J Am Chem Soc*. 2016; 138:3058–3065. [PubMed: 26859432]
75. Suslov NB, DasGupta S, Huang H, Fuller JR, Lilley DMJ, Rice PA, Piccirilli JA. Crystal structure of the Varkud satellite ribozyme. *Nat Chem Biol*. 2015; 11:840–846. [PubMed: 26414446]
76. Ren A, Vusurovic N, Gebetsberger J, Gao P, Juen M, Kreutz C, Micura R, Patel DJ. Pistol ribozyme adopts a pseudoknot fold facilitating site-specific in-line cleavage. *Nat Chem Biol*. 2016; 12:702–708. [PubMed: 27398999]
77. Wilson TJ, Liu Y, Domnick C, Kath-Schorr S, Lilley DMJ. The Novel Chemical Mechanism of the Twister Ribozyme. *J Am Chem Soc*. 2016; 138:6151–6162. [PubMed: 27153229]
78. Pinard R, Hampel KJ, Heckman JE, Lambert D, Chan PA, Major F, Burke JM. Functional involvement of G8 in the hairpin ribozyme cleavage mechanism. *EMBO J*. 2001; 20:6434–6442. [PubMed: 11707414]
79. Han J, Burke JM. Model for General Acid–Base Catalysis by the Hammerhead Ribozyme: pH-Activity Relationships of G8 and G12 Variants at the Putative Active Site. *Biochem*. 2005; 44:7864–7870. [PubMed: 15910000]
80. Liu H, Yu X, Chen Y, Zhang J, Wu B, Zheng L, Haruehanroengra P, Wang R, Li S, Lin J, Li J, Sheng J, Huang Z, Ma J, Gan J. Crystal structure of an RNA-cleaving DNAzyme. *Nat Commun*. 2017; 8:2006. [PubMed: 29222499]

**Figure 1.**

A) A schematic representation of the secondary structure of the 8-17 DNAzyme (green strand) and its substrate (black strand).³¹ The cleavage site is indicated by a red arrow. Blue nucleotides indicate catalytically relevant guanines analyzed in this study. B) Guanine analogs used in this study and the pK_a of N1 for each of them.

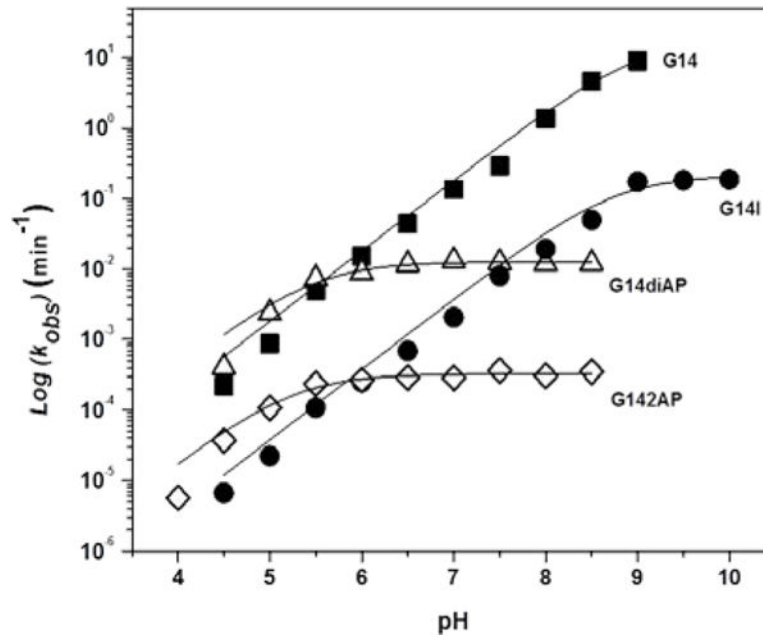


Figure 2. pH profile of 17E and 17E-G14 analogs. (■)17S/E wild type, (●)17E-G14I, () 17E-G14diAP, ()17E-G14AP. The rate-pH profile of 17E DNAzyme was fit to the equation $k_{obs} = k_{max} / [1 + 10^{(pK_a - pH)}]$.^{56, 78, 79}

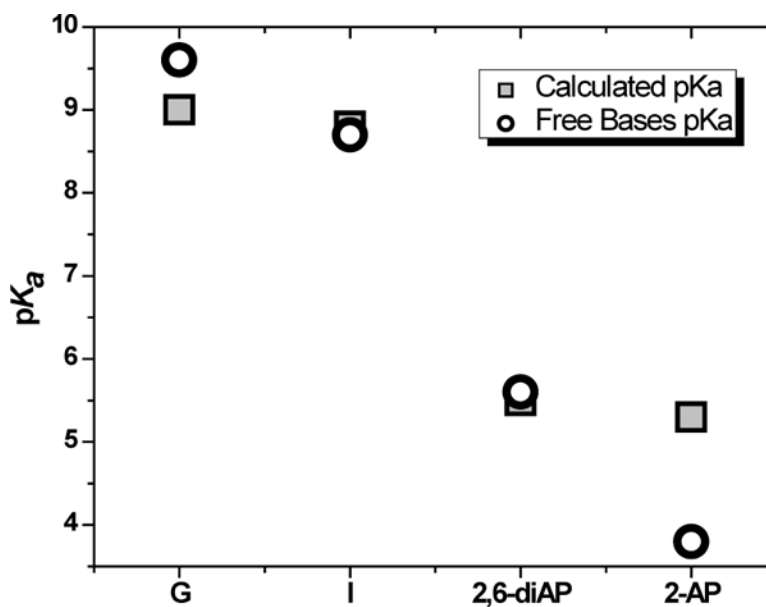


Figure 3. pK_a values of the N1 proton of the 8-17 DNAzyme and G14 variants. White circles indicate the pK_a of free bases and grey squares show the calculated pK_a of the G14 analogues in the 8-17 DNAzyme based upon the pH-rate profiles using the equation $k_{obs} = k_{max} / [1 + 10^{(pK_a - pH)}]$.^{56, 78, 79}

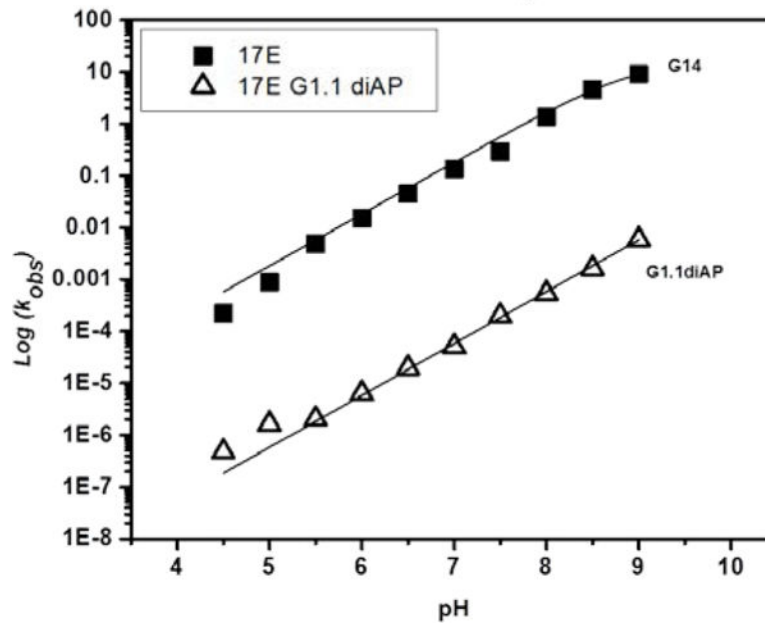


Figure 4. Rate-pH profile of 17E wild type (■) and 17E/S-G1.1diAP (△). The rate-pH profile of the 8-17 DNAzyme was fit to the equation $k_{obs} = k_{max} / [1 + 10^{(pK_a - pH)}]$.^{56, 78, 79}